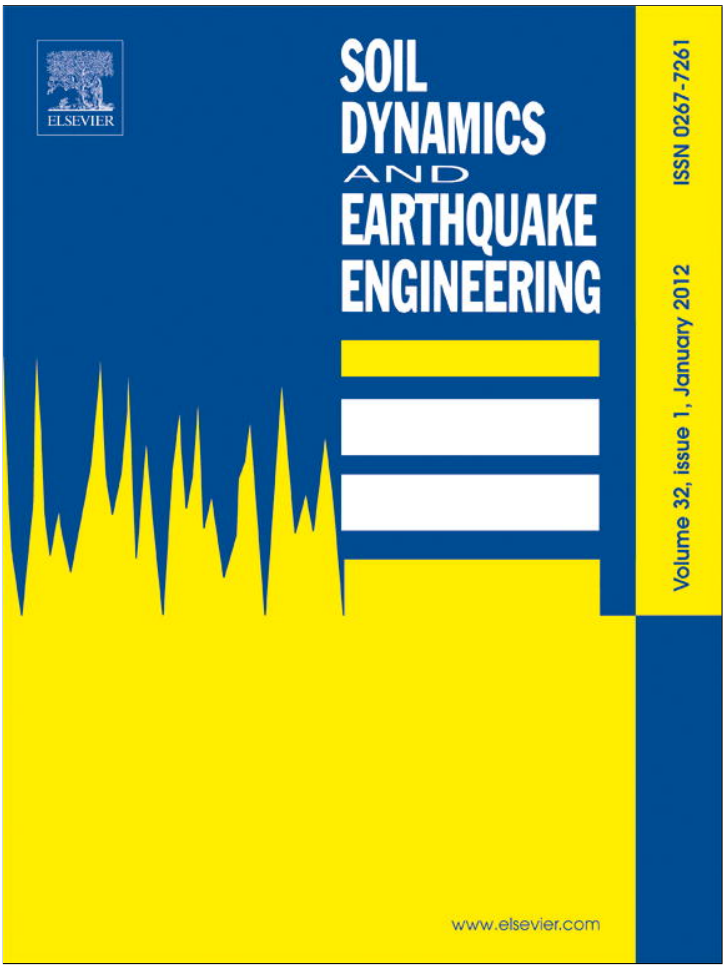

Soil Dynamics and Earthquake Engineering 51 (2013) 14–22

Contents lists available at SciVerse ScienceDirect

Soil Dynamics and Earthquake Engineering

journal homepage: www.elsevier.com/locate/soildyn

Ant colony optimization of tuned mass dampers for earthquake oscillations of high-rise structures including soil–structure interaction

Anooshiravan Farshidianfar, Saeed Soheili *

Mechanical Engineering Department, Ferdowsi University of Mashhad, Mashhad, Iran

ARTICLE INFO

Article history:
Received 20 April 2011
Received in revised form
13 March 2013
Accepted 6 April 2013

Keywords:
High-rise structures
Earthquake oscillations
Tuned mass dampers
Ant colony optimization
Soil–structure interaction

ABSTRACT

This paper investigates the optimized parameters for tuned mass dampers (TMDs) to decrease the earthquake vibrations of tall buildings; involving soil–structure interaction (SSI) effects. The time domain analysis based on Newmark method is employed in this study. To illustrate the results, Tabas and Kobe earthquakes data are applied to the model, and ant colony optimization (ACO) method is utilized to obtain the best parameters for TMD. The TMD mass, damping coefficient and spring stiffness are assumed as design variables, and the objective is to reduce both the maximum displacement and acceleration of stories. It is shown that how the ACO can be effectively applied to design the optimum TMD device. It is also indicated that the soil type greatly affects the TMD optimized parameters and the time response of structures. This study helps the researchers to better understanding of earthquake vibrations, and leads the designers to achieve the optimized TMD for high-rise buildings.

1. Introduction

In recent years, the construction of new high-rise buildings are facilitated and developed in many countries due to the lighter and stronger materials. Since these structures are usually subjected to the earthquake vibrations, the study of tall buildings vibration mitigation and various absorbers has attracted the interest of many researchers. The tuned mass damper (TMD) is one of the simplest and the most reliable control devices among the numerous passive control methods. The main idea of employing a TMD is to produce a supplementary system that can absorb energy from the main system. The TMD technology uses a mass–spring system which oscillates with the structure, and an additional damper that connects two relatively moving points when the building oscillates. In this way, a large amount of the structural vibrating energy is transferred to the TMD and then dissipated by the damping as the primary structure is subjected to external disturbances, like earthquake and wind oscillations.

This system absorbs the vibrations automatically, and in this way the safety of the structure are greatly improved and the protected system can endure excessive vibrations and loading episodes, which can result in damage and even in failure of structural elements and equipment in the absence of TMD.

Many researchers have studied the applicability of TMDs for structures subjected to seismic excitation such as Villaverde and Koyoama [1], Rana and Soong [2], Lin et al. [3] and Wang et al. [4].

In order to develop the efficiency of control strategy, it is important to find the optimum mechanical parameters (i.e. the optimum tuning frequency, damping and mass ratio) of TMD. Several design formulas for the optimum parameters of a TMD, for different types of oscillations, have been proposed. Brock [5] and Den Hartog [6] explained the estimation of the optimum parameters of the TMD for an undamped structure subjected to harmonic external excitation. Since then, many optimum design methods of TMD have been developed to control the structural vibrations induced by various types of excitation sources, such as Crandall and Mark [7], and Rana and Soong [2]. On the basis of Den Hartog's method, Warburton and Ayorinde [8] obtained the optimized parameters of the TMD for an undamped structure under harmonic support excitation, where the acceleration amplitude is set to be constant for all input frequencies, and also for other kinds of harmonic excitations. Later, Sadek et al. [9] presented some formulations for computing the optimal parameters of TMD device based on the equal damping of the first two modes of system.

However, the optimum parameters of TMD are determined through parametric studies, or by their proposed optimum design methods. Moreover, the external disturbances considered in these studies are usually limited to white noise and harmonic forces over a frequency range. Actually, random signals such as earthquake excitations; are considered in few works, such as references [9,10].

* Corresponding author. Tel.: +98 511 8763304.
E-mail addresses: farshid@um.ac.ir (A. Farshidianfar), soheili78@yahoo.com, sa_so107@stu-mail.um.ac.ir (S. Soheili).

0267-7261/$ - see front matter © 2013 Elsevier Ltd. All rights reserved.
http://dx.doi.org/10.1016/j.soildyn.2013.04.002

In fact, many structures are built on soft soil where the soil–structure interaction (SSI) effect may be significant. It is well known that the SSI effects would significantly modify the dynamic characteristics of structures such as natural frequencies, damping ratios and mode shapes [11]. Xu and Kwok [12] investigated the wind-induced motion of two tall structures mounted with TMD, considering the effect of soil compliancy under the footing. They believed that soil compliancy will affect structural responses as well as the TMD effectiveness. Wu et al. [13] focused on the TMD seismic performance for structures of shallow foundations. They performed numerical investigations for a specific TMD–structure (with height of 45 m) system built on soils with various shear wave velocities. Recently, Liu et al. [14] developed a mathematical model for time domain analysis of wind induced oscillations of a tall building with TMD considering soil effects.

However, the proposed elastic half-space model without considering material damping for soil which was not satisfied for seismic application was questionable. Moreover, the past studies on TMD used for seismic applications in structures, have not considered the effects of the altered properties of the structure due to SSI, on the performance of the damper.

Another device for decreasing the earthquake induced vibration of structures is multiple tuned mass damper (MTMD), which consists of different mass–spring systems with tuned frequencies. Wang and Lin [15] investigated the effect of MTMDs on the vibration control of irregular buildings modeled as torsionally coupled structures including SSI effects. They concluded that both the SSI and eccentricity effects should be regarded for determination of optimal MTMD parameters to avoid overestimation of its effectiveness. The study of active control system for an irregular building shows that the SSI effect is significant for both squatty and slender buildings, as Lin et al. [16] considered. Therefore, the soil–structure interaction should be considered for the design of active control devices; especially for high-rise buildings. Lin et al. also [17] proposed a novel semi-active friction-type multiple tuned mass damper (SAF-MTMD) for vibration control of seismic structures.

According to Li [18], when an asymmetric structure is built on soft soil sites, the effectiveness and robustness of the active MTMD for asymmetric structures is overestimated or underestimated if the SSI effect is neglected. Li and Han [19] indicated that the dominant ground frequency and soil characteristics have important influences on the optimum parameters, effectiveness and stroke displacement of the MTMD; and the MTMD can be applied to the structures with the controlled natural frequency less than dominant earthquake frequency. They also implied that the dominant frequency of ground motion has slightly smaller effect on the performance of the MTMD in the case of suppressing the structural acceleration response in contrast with the case of controlling the displacement response. According to Li and Liu [20], the earthquake ground motion can be represented by a white noise for the optimum design of MTMD; where both the total mass ratio is lower than 0.02 and the total mass ratio is over 0.02 but the dominant frequency of earthquake is above the frequency of structure. Li et al. [21] also investigated the influences of various parameters in the soil–asymmetric structure interaction system on both the effectiveness and robustness of the active TMD and MTMD.

Although numerous works are performed concerning SSI effects, few investigations are carried out on the time response of high-rise buildings due to earthquake excitations. In fact, the earthquake time response of tall buildings has usually been calculated employing fixed base models or single degree of freedom (SDOF) system. These analyzes cannot reasonably predict the structural responses. Moreover, the optimal parameters of TMD are extremely related to the soil type. Therefore, the time domain analysis of structures consisting SSI effects is an advantageous process for the better understanding of earthquake oscillations and TMD devices. Furthermore, few works have considered and employed heuristic algorithms, while the heuristic techniques such as ant colony optimization (ACO) method, can be effectively employed for the optimized design of TMDs.

In this paper, a mathematical model is developed for calculating the earthquake response of a high-rise building with TMD. The model is employed to obtain the time response of 40 story building using TMD. The ant colony optimization (ACO) method is applied on the model to obtain the best TMD parameters. The parameters are calculated with and without soil–structure interaction (SSI) effects. The effects of different parameters such as mass, damping coefficient, spring stiffness, natural frequency and damping ratio are investigated.

2. Modeling of high-rise structures

Fig. 1 shows a N-story structure with a TMD and SSI effects. Mass and moment of inertia for each floor are indicated as M_i and I_i, and those of foundation are shown as M_0 and I_0, respectively. The stiffness and damping between floors are assumed as K_i and C_i, respectively. M_{TMD}, K_{TMD} and C_{TMD} are the related parameters for TMD. Damping of the swaying and rocking dashpots are represented as C_s and C_r, and the stiffness of corresponding springs are indicated as K_s and K_r, respectively. Time histories of displacement and rotation of foundation are respectively defined as X_0 and θ_0, and displacement of each story is shown as X_i.

Using Lagrange's equation, the equation of motion for a building shown in Fig. 1 can be represented as follows [22]:

$$[m]\ddot{x}(t) + [c]\dot{x}(t) + [k]x(t) = -[m^*]\{1\}\ddot{u}_g \quad (1)$$

where $[m]$, $[c]$ and $[k]$ denote mass, damping and stiffness of the oscillating system, respectively. $[m^*]$ indicates acceleration mass matrix for earthquake and $\ddot{u}_g$ is the earthquake acceleration. Considering SSI effects, the N-story structure is a N+3 degree-of-freedom oscillatory system. For such building, the mass matrix is obtained by employing Lagrange's equation in the

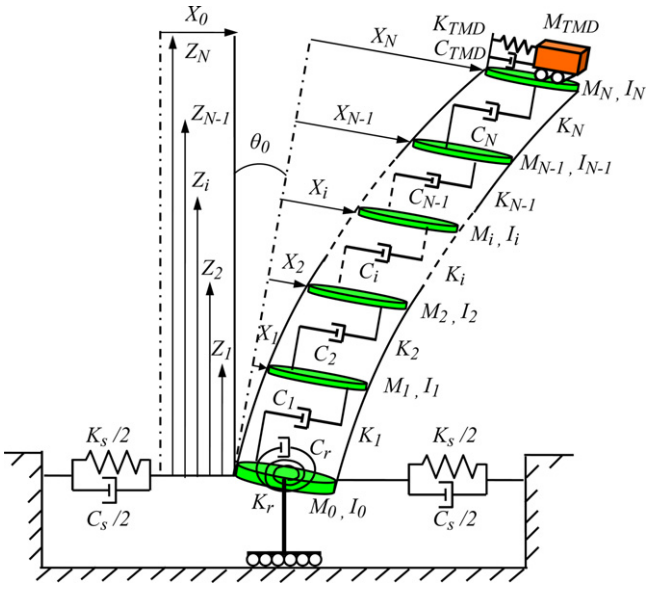

Fig. 1. Shear building configuration.

following form [14,22]:

$$[m]=\begin{bmatrix} [M]_{N\times N} & \{0\}_{N\times 1} & [M]_{N\times 1} & [MZ]_{N\times 1} \\ & M_{TMD} & M_{TMD} & M_{TMD}Z_N \\ & & M_0+\sum_{j=1}^{N}M_j+M_{TMD} & \sum_{j=1}^{N}M_jZ_j+M_{TMD}Z_N \\ symmetry & & & I_0+\sum_{j=1}^{N}(I_j+M_jZ_j^2)+M_{TMD}Z_N^2 \end{bmatrix} \tag{2}$$

where

$$[M]_{N\times N}=\begin{bmatrix} M_1 & 0 & 0 & 0 & 0 \\ & M_2 & 0 & 0 & 0 \\ & & \ldots & \{0\} & \{0\} \\ & & & M_{N-1} & 0 \\ symmetry & & & & M_N+M_{TMD} \end{bmatrix} \tag{3}$$

$$[M]_{N\times 1}=\begin{bmatrix} M_1 \\ M_2 \\ \vdots \\ M_{N-1} \\ M_N+M_{TMD} \end{bmatrix} \tag{4}$$

$$[MZ]_{N\times 1}=\begin{bmatrix} M_1Z_1 \\ M_2Z_2 \\ \vdots \\ M_{N-1}Z_{N-1} \\ (M_N+M_{TMD})Z_N \end{bmatrix} \tag{5}$$

Using Lagrange's equation, the stiffness matrix is achieved as follows [14,22]:

$$[k]=\begin{bmatrix} [K]_{N\times N} & 0_{N\times 1} & 0_{N\times 1} & 0_{N\times 1} \\ & K_{TMD} & 0 & 0 \\ & & K_s & 0 \\ symmetry & & & K_r \end{bmatrix} \tag{6}$$

in which

$$[K]_{N\times N}=\begin{bmatrix} K_1+K_2 & -K_2 & 0 & 0 & 0 \\ & K_2+K_3 & 0 & 0 & 0 \\ & & \cdots & \vdots & \{0\} \\ & & & K_{N-1}+K_N & -K_N \\ symmetry & & & & K_N \end{bmatrix} \tag{7}$$

Similarly, the damping matrix can be stated in the following form:

$$[c]=\begin{bmatrix} [C]_{N\times N} & 0_{N\times 1} & 0_{N\times 1} & 0_{N\times 1} \\ & C_{TMD} & 0 & 0 \\ & & C_s & 0 \\ symmetry & & & C_r \end{bmatrix} \tag{8}$$

where

$$[C]_{N\times N}=\begin{bmatrix} C_1+K_2 & -C_2 & 0 & 0 & 0 \\ & C_2+C_3 & 0 & 0 & 0 \\ & & \cdots & \vdots & \{0\} \\ & & & C_{N-1}+C_N & -C_N \\ symmetry & & & & C_N \end{bmatrix} \tag{9}$$

Finally, the acceleration mass is obtained as follows:

$$[m^*]=\begin{bmatrix} [M]_{N\times N} & \{0\}_{N\times 1} & 0_{N\times 1} & 0_{N\times 1} \\ 0 & M_{TMD} & 0 & 0 \\ 0 & 0 & M_0+\sum_{j=1}^{N}M_j+M_{TMD} & 0 \\ 0 & 0 & \sum_{j=1}^{N}M_jZ_j+M_{TMD}Z_N & 0 \end{bmatrix} \tag{10}$$

Ignoring the SSI effects, rows and columns N+2 and N+3 are neglected, and the mentioned matrices are reduced to $(N+1)\times(N+1)$ dimensional matrices.

According to Rayleigh proportional damping, the damping matrix of N-story structure can be represented as follows:

$$[c]_{N\times N}=A_0[m]_{N\times N}+A_1[k]_{N\times N} \tag{11}$$

in which A_0 and A_1 are Rayleigh damping coefficients.

The displacement vector $\{x(t)\}$ including both displacement and rotation of floors and foundation as well as TMD motion can be represented as follows:

$$x(t)=X_1(t)\quad X_2(t)\quad \ldots\quad X_N(t)\quad X_{TMD}(t)\quad X_0(t)\quad \theta_0(t)^T \tag{12}$$

The parameters C_s, C_r, K_s and K_r can be obtained from soil properties (i.e. Poisson's ratio υ_s, density ρ_s, shear wave velocity V_s and shear modulus G_s) and radius of foundation R_0 [14].

In this paper, Tabas and Kobe earthquakes acceleration spectra are applied to the structure, and time response of TMD and building are calculated based on Newmark integration method [23].

3. Ant colony optimization (ACO)

In order to obtain the best parameters for TMD, the ant colony optimization (ACO) is employed. This algorithm firstly proposed by Dorigo and Gambardella [24] is based on the behavior of ants finding the shortest paths from a food source to their nest only by sensing the intensity of pheromone deposited by other ants. It is observed that they usually select the path with higher pheromone. This mechanism makes the shorter paths more desirable as it takes shorter time to march on them.

This behavior is simulated by three rules in ACO algorithm, which was originally applied on combinatorial problems with discrete variables such as Traveling Salesman or Quadratic Assignment. For engineering problems where the design variables are usually continuous, the method of discretization is an acceptable approach [25]. Once the continuous variables are divided into separated domains, the problem can be treated as a problem with discrete variables.

Regarding the discretization procedure, the design variables are presented by i and their divided search domains are shown by j. The sections of total solution are chosen in a constructive approach named as "state transition rule":

$$S=\begin{cases} \arg\max\left\{ [\tau(i,j)]\,.\,[\eta(i,j)]^{\beta} \right\} & \text{if } q\le q_0 \\ s & \text{otherwise} \end{cases} \tag{13}$$

where $\tau(i,j)$ shows the amount of pheromone related to the jth element of variable i, and $\eta(i,j)$ is the heuristic function defined according to the investigated problem. In this rule, q is a random number, and q_0 is a parameter set by the user ($0\le q, q_0\le 1$). If $q > q_0$, the next step is selected according to proportional distribution of probability function, like the roulette wheels, assigned as follows:

$$s=\begin{cases} \dfrac{[\tau(i,j)]\,.\,[\eta(i,j)]^{\beta}}{\sum_{u\in\ allowed\ u}[\tau(i,u)]\,.\,[\eta(i,u)]^{\beta}} & \text{if } j\in \text{allowed } j \\ 0 & \text{otherwise} \end{cases} \tag{14}$$

The significant factor of q_0 defines the range of randomness against determination of state transition rule. It is clear that the higher amount of q_0 directs the algorithm towards deterministic decisions, while the lower amounts generates more randomness.

To avoid stagnation of the algorithm and similar to evaporation of pheromone in real world, the amount of pheromone level is changed after finishing each evaluation by applying "the local updating rule":

$$\tau(i,j)=(1-\rho).\tau(i,j)+\rho.\Delta\tau(i,j) \tag{15}$$

where ρ denotes the local evaporation coefficient. The best performance is obtained when $\Delta\tau(i,j)=\tau_0$ [24].

The third rule known as "the global updating rule" acts as a positive feedback and accumulates more pheromone around the best solution obtained so far:

$$\tau(i,j)=(1-\alpha).\tau(i,j)+\alpha.\Delta\tau \tag{16}$$

where $\Delta\tau$ is the inverse of the objective function and α is the global evaporation coefficient [24].

This process of evaluation and updating is repeated with n ants until the termination condition, which is usually the maximum number of cycles, is satisfied. Similar to other heuristic optimization techniques, it is important to tune the algorithm to achieve sensible results. For the tackled problem in this paper, the values presented in Table 1 are found acceptable. In addition, without damaging the overall effectiveness of ACO [24], the heuristic function is neglected due to intricacies in its definition procedure.

Table 1
ACO parameter settings.

n	α	ρ	τ_0	q_0
5	0.1	0.1	2	0.75

Since the problem is of multi-objective nature trying to minimize both the maximum displacement and acceleration of the building, an overall objective function including both concepts should be employed. Here, as the acceleration results are nearly 10 times greater than displacement, the objective function is defined as follows:

$$f_i=\ddot{u}_{\max}+10u_{\max} \tag{17}$$

where $u_{\max}$ and $\ddot{u}_{\max}$ denotes the maximum displacement and acceleration values, respectively. Fig. 2 shows the flowchart of ACO algorithm employed for TMD optimization.

4. Illustrative example

The methodology outlined previously is employed to calculate the structural response of a 40-story building with TMD. Table 2 shows the structure parameters [14]. The stiffness K_i linearly decreases as Z_i increases. TMD is installed on the top of building for the better damping of vibrations.

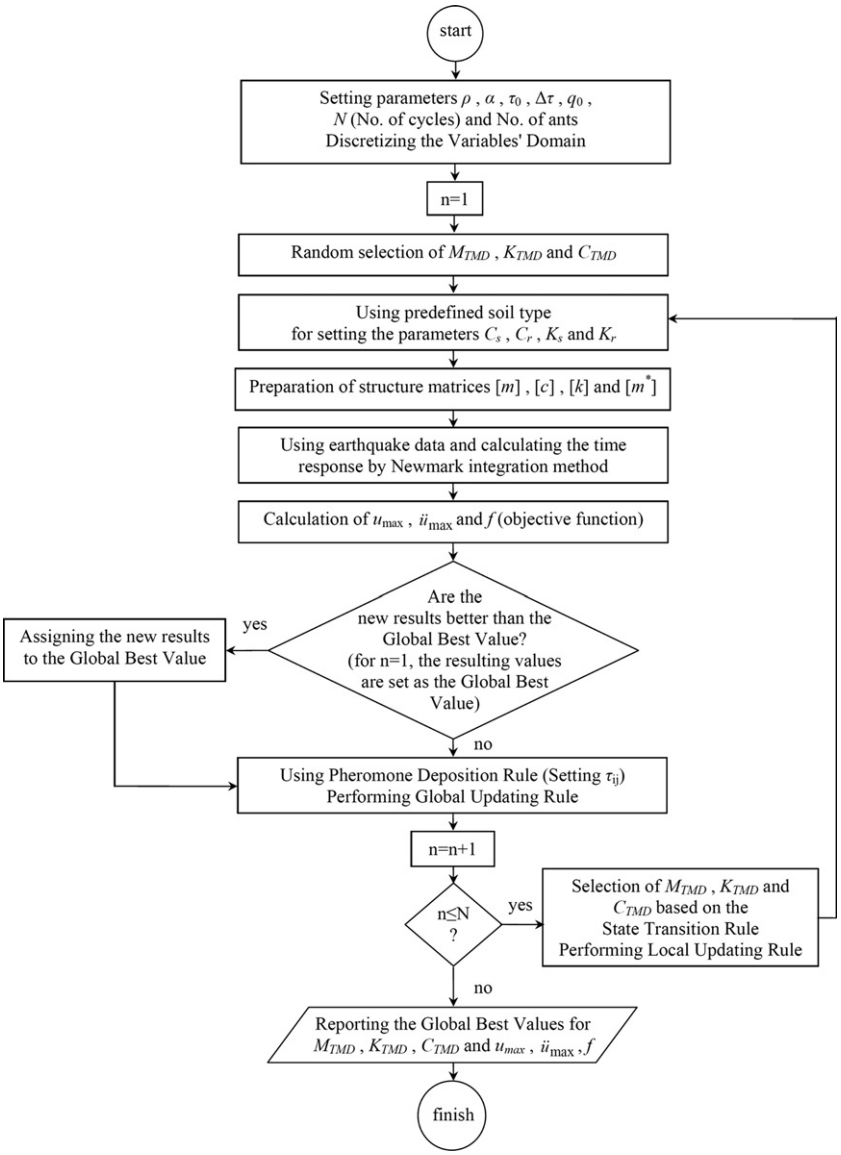

Fig. 2. Flowchart of ACO algorithm.

Table 2
Structure parameters [14].

No. of stories	40
Story height (Z_i)	4 m
Story mass (M_i)	9.8×10^5 kg
Story moment of inertia (I_i)	1.31×10^8 kgm^2
Story stiffness (K_i)	$K_1=2.13\times10^9$ N/m $K_{40}=9.98\times10^8$ N/m $K_{40}\le K_i\le K_1$
Foundation radius (R_0)	20 m
Foundation mass (M_0)	1.96×10^6 kg
Foundation moment of inertia (I_0)	1.96×10^8 kgm^2

Table 3
Parameters of the soil and foundation.

Soil type	Swaying damping C_s (Ns/m)	Rocking damping C_r (Ns/m)	Swaying stiffness K_s (N/m)	Rocking stiffness K_r (N/m)
Soft soil	2.19×10^8	2.26×10^{10}	1.91×10^9	7.53×10^{11}
Medium soil	6.90×10^8	7.02×10^{10}	1.80×10^{10}	7.02×10^{12}
Dense soil	1.32×10^9	1.15×10^{11}	5.75×10^{10}	1.91×10^{13}

Table 4
Natural and damped frequencies of the structure.

Soil type	ω	ω_1 (rad/s)	ω_2 (rad/s)	ω_3 (rad/s)
1 Soft soil	With damping	$-0.02i\pm1.08$	$-0.24i\pm4.45$	$-0.62i\pm7.42$
	Without damping	1.09	4.44	7.40
2 Medium soil	With damping	$-0.02i\pm1.54$	$-0.21i\pm4.57$	$-0.58i\pm7.55$
	Without damping	1.54	4.58	7.58
3 Dense soil	With damping	$-0.02i\pm1.60$	$-0.21i\pm4.58$	$-0.58i\pm7.57$
	Without damping	1.61	4.59	7.59
4 Fixed base	With damping	$-0.03i\pm1.64$	$-0.21i\pm4.59$	$-0.58i\pm7.58$
	Without damping	1.65	4.60	7.60

In this study, three types of ground states, namely soft, medium and dense soil are examined. A structure with a fixed base is also investigated. The soil and foundation properties are presented in Table 3.

Table 4 represents the first 3 natural and damped frequencies of the structure, considering and ignoring SSI effects. The TMD design variables are set in such a way that all the first 3 frequencies of the structure are covered, and damping ratio (ξ) is always less than unity. In this way, the maximum mass ratio is about 6.5% of the first modal mass, i.e. $100\times10^3\le M_{TMD}\le2000\times10^3$ (kg), the TMD spring stiffness is set as $0.5\times10^6\le K_{TMD}\le60\times10^6$ (N/m) and the TMD damping is tuned to $0.1\times10^3\le C_{TMD}\le2000\times10^3$ (Ns/m).

As mentioned before, Tabas and Kobe earthquakes data are employed to obtain the optimized mass, damping and stiffness for TMD device. The objective is to decrease the maximum displacement and acceleration of structure during earthquake oscillation. Therefore, it should be treated as a multi-objective optimization problem.

5. Results and discussions

The optimized mass, spring stiffness and damping coefficient of TMD obtained by ACO are presented in Figs. 3, 4 and 5, respectively; for Tabas and Kobe earthquakes. Figs. 6, 7 and 8, respectively show the natural and damped frequency and damping ratio of TMD.

The results show that there is a close relationship between soil and optimized parameters of TMD. According to Figs. 3, 4 and 5, the structure constructed on the soil with greater stiffness and damping needs TMD with smaller M_{TMD}, K_{TMD} and C_{TMD}. Therefore,

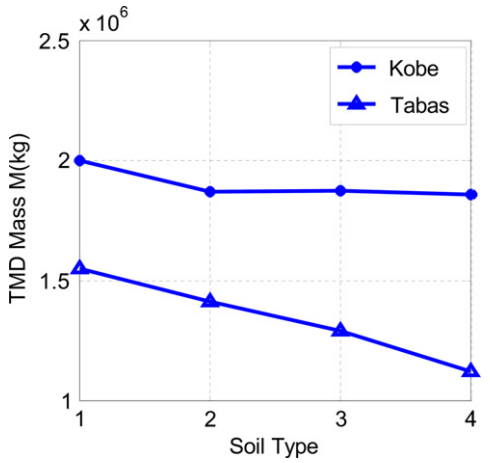

Fig. 3. Optimized M_{TMD} for 4 soil types.

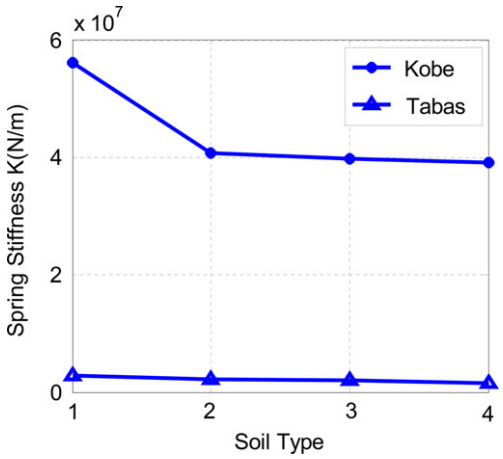

Fig. 4. Optimized K_{TMD} for 4 soil types.

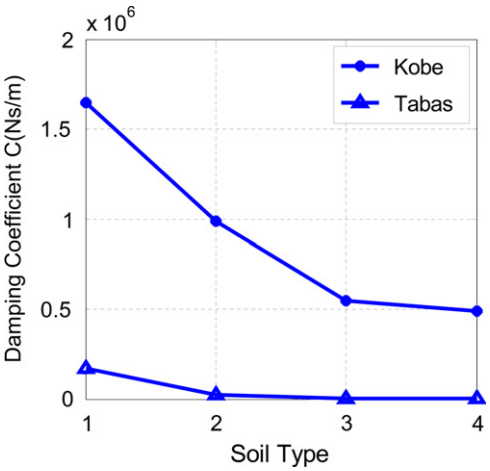

Fig. 5. Optimized C_{TMD} for 4 soil types.

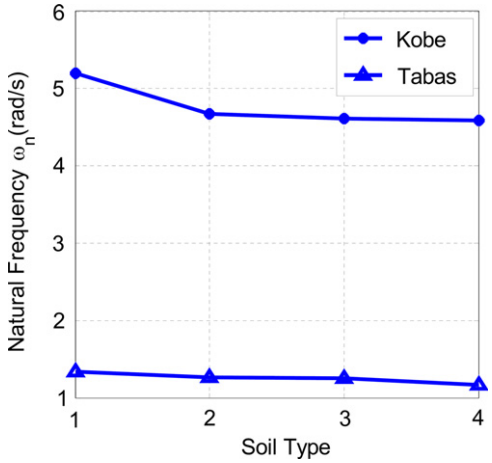

Fig. 6. Optimized ω_n for 4 soil types.

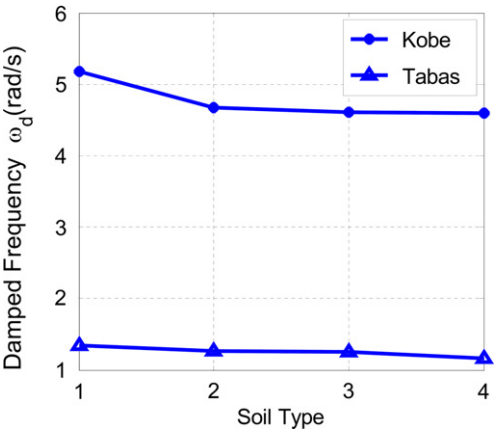

Fig. 7. Optimized ω_d for 4 soil types.

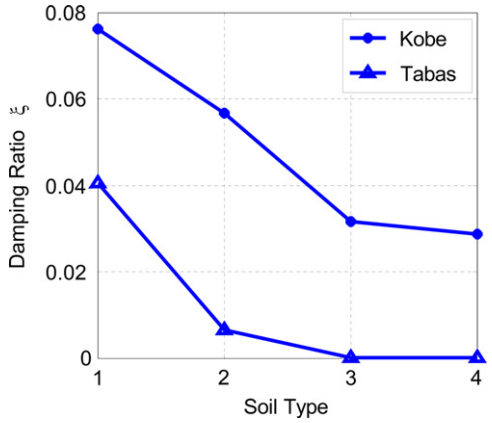

Fig. 8. Optimized ξ for 4 soil types.

the proper TMD for the dense soil is the one with lower ω_n, ω_d and ξ, as illustrated in Figs. 6, 7 and 8. Considering Table 4, the soil with higher stiffness and damping brings higher natural and damped frequency, therefore; it can be concluded that the structure with higher frequency (constructed on the dense soil) requires TMD with lower frequency. Furthermore, the study of damping ratio reveals that the structure on the dense soil (with greater frequency and smaller damping) needs TMD with lower damping ratio.

The mentioned figures also reveal that the TMD values obtained for Tabas earthquake are smaller than Kobe in all cases. Comparing fixed base model with other three models indicates

Table 5
Vibration with and without TMD for Tabas earthquake.

Soil type	Without TMD		With TMD		% Reduction		% Reduction for target function
	u_{max} (m)	$\ddot{u}_{max}$ (m/s^2)	u_{max} (m)	$\ddot{u}_{max}$ (m/s^2)	u_{max}	$\ddot{u}_{max}$	
Soft soil	4.2291	12.2094	2.9509	12.2714	30.23	0.51	23.34
Medium soil	2.6733	12.8245	1.6592	12.7974	37.93	0.21	25.70
Dense soil	2.2642	12.8148	1.4290	12.7798	36.88	0.27	23.65
Fixed base	2.0235	12.7756	1.4135	12.7507	30.14	0.19	18.54

Table 6
Vibration with and without TMD for Kobe earthquake.

Soil type	Without TMD		With TMD		% Reduction		% Reduction for target function
	u_{max} (m)	$\ddot{u}_{max}$ (m/s^2)	u_{max} (m)	$\ddot{u}_{max}$ (m/s^2)	u_{max}	$\ddot{u}_{max}$	
Soft soil	0.7588	9.5493	0.6819	8.8428	10.13	7.40	8.61
Medium soil	1.0615	11.2907	0.8247	8.5901	22.31	23.92	23.14
Dense soil	1.0576	11.4019	0.8632	8.8109	18.38	22.72	20.63
Fixed base	1.0459	11.4408	0.9318	8.8322	10.90	22.8	17.12

that ignoring the soil characteristics would result in the underestimation of TMD's frequency and damping ratio.

Tables 5 and 6 respectively show the values of maximum displacement and acceleration for Tabas and Kobe earthquakes, considering and ignoring TMD. According to Table 5, the maximum feasible reduction for the building displacement is much greater than its acceleration. It means that the TMD is more effective for the reduction of displacement than acceleration. However, Table 6 indicates that the reduction amount of building's displacement and acceleration are nearly the same for Kobe earthquake.

Furthermore, it can be seen that the soil type brings important effects on the structure vibrations. Generally, the soil with higher stiffness reduces the maximum displacement and acceleration (except for the soft soil in some cases), and decreases the maximum possible reduction in most cases. It implies that the TMDs are less effective for dense soils. Comparing fixed base model with other three models reveals that ignoring the soil characteristics usually brings the underestimation of the maximum displacement, acceleration and possible reduction.

Fig. 9 shows Tabas earthquake acceleration spectrum, which was about 7.7 Richter and occurred in 16th September 1978 in Tabas, Iran. Fig. 10 shows the frequency spectrum of Tabas earthquake acceleration. According to this figure, the most effective frequency is $\omega=1.381$ (rad/s), which explains that why the optimized TMD frequencies are obtained nearly $\omega_n=1.15$–1.35 (rad/s); as mentioned in Fig. 6.

Kobe earthquake was about 6.7 Richter and occurred in 16th January 1995 in Kobe, Japan. The earthquake acceleration and its frequency spectra are presented in Figs. 11 and 12, respectively. Considering Fig. 12, the most effective frequency is between $\omega=2.915$(rad/s) and $\omega=5.139$ (rad/s), which explains that why the optimized TMD frequencies are obtained nearly $\omega_n=4.50$–5.20 (rad/s); as mentioned in Fig. 6.

Since the TMD system should work at single frequency, the effects of Kobe TMD settings using Tabas earthquake and also Tabas TMD settings employing Kobe earthquake are investigated, and the results are presented in Tables 7 and 8; respectively. According to Table 7, it can be seen that the TMD actually increases the displacement in most cases, while the results of Table 8 reveals that the TMD device decreases the maximum displacement and acceleration, although it is not as effective as the optimized one

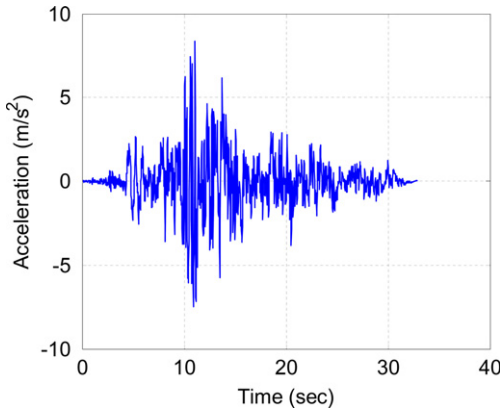

Fig. 9. Tabas seismic acceleration spectrum.

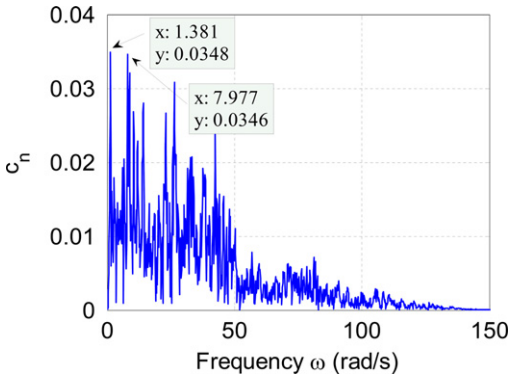

Fig. 10. Tabas seismic frequency spectrum.

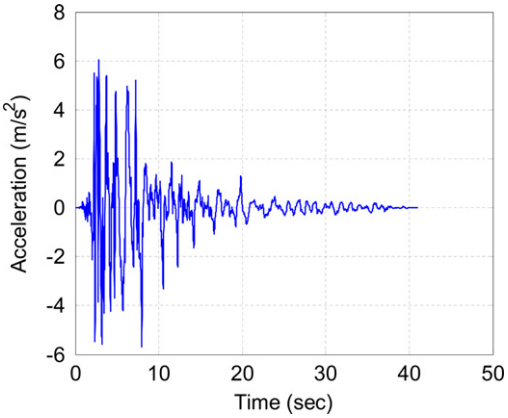

Fig. 11. Kobe seismic acceleration spectrum.

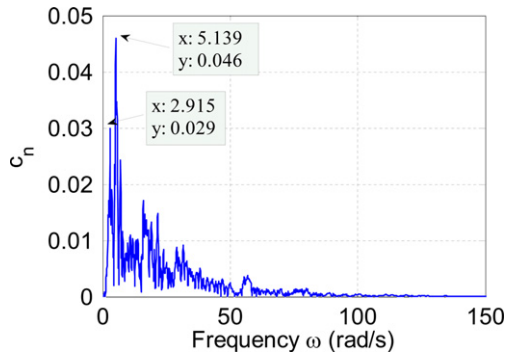

Fig. 12. Kobe seismic frequency spectrum.

mentioned in Table 5. It can be concluded that by setting the TMD frequency near the first natural frequency of the structure, the seismic response due to the both earthquakes (with main frequencies near the first and second frequency of the building) would be deceased, while tuning the TMD frequency near the second natural frequency of the structure would bring not acceptable results for the seismic excitations with the main frequency near the first natural frequency of the structure. Therefore, the TMD frequency is to be set close to the first natural frequency of the structure.

Regarding Tabas earthquake, Figs. 13 and 14 represent the effects of TMD's spring stiffness and damping coefficient on the displacement and acceleration, respectively; employing the medium soil and for $M=1.411\times10^6$ (kg) (the optimized mass). Fig. 13 reveals that the optimum results are obtained when C is decreased and $K\approx2.25\times\times10^6$ (N/m). Considering Fig. 14, it is clear that the acceleration is reduced by increasing the spring stiffness.

The effects of TMD's spring stiffness and mass on the displacement and acceleration are presented in Figs. 15 and 16, respectively; using the medium soil and $C=0.023\times10^6$ (Ns/m). Fig. 15 indicates that the minimum displacement yields when the spring stiffness approaches $K\approx2.25\times10^6$ (N/m), as mentioned previously. It is also clear that increasing the TMD's mass would increase the displacement generally, except for the values near the optimum

Table 7
Vibration with and without TMD for Tabas earthquake with kobe TMD settings.

Soil type	Without TMD		With TMD		% Reduction		% Reduction for target function
	u_{max} (m)	$\ddot{u}_{max}$ (m/s²)	u_{max} (m)	$\ddot{u}_{max}$ (m/s²)	u_{max}	$\ddot{u}_{max}$	
Soft soil	4.2291	12.2094	3.8470	12.1748	9.04	0.28	7.07
Medium soil	2.6733	12.8245	3.5388	12.5676	−32.38	2.00	−21.23
Dense soil	2.2642	12.8148	2.7844	12.6927	−22.98	0.95	−14.33
Fixed base	2.0235	12.7756	2.5476	12.7312	−25.90	0.35	−15.74

Table 8
Vibration with and without TMD for Kobe earthquake with Tabas TMD settings.

Soil type	Without TMD		With TMD		% Reduction		% Reduction for target function
	u_{max} (m)	$\ddot{u}_{max}$ (m/s²)	u_{max} (m)	$\ddot{u}_{max}$ (m/s²)	u_{max}	$\ddot{u}_{max}$	
Soft soil	0.7588	9.5493	0.7227	9.5354	4.76	0.15	2.19
Medium soil	1.0615	11.2907	0.9869	11.2384	7.03	0.46	3.64
Dense soil	1.0576	11.4019	0.9884	11.3303	6.54	0.63	3.47
Fixed base	1.0459	11.4408	0.9958	11.3851	4.79	0.49	2.54

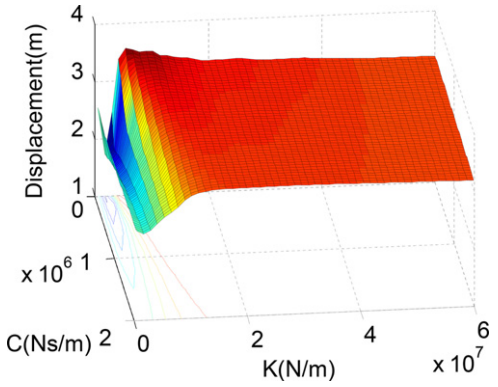

Fig. 13. The effects of TMD's C and K on u_{max}.

spring stiffness, i.e. $K \approx 2.25 \times 10^6$ (N/m). Considering Fig. 16, it is evident that the best results are obtained through the line that brings $\omega_n \approx 1.3$ (rad/s). Obviously, the acceleration is increased out of this line.

Figs. 17 and 18 show the time response of structure with and without TMD for the soft soil, and Figs. 19 and 20 represent those for the dense soil; respectively; due to Tabas earthquake oscillations. It can be seen that the maximum displacement is reduced due to the TMD device. Comparing Figs. 17 and 18, it is evident that the displacement patterns of the structure are nearly different in the mentioned figures, but the TMD displacement pattern is nearly similar to the structure. The TMD amplitude is about 4 times greater than the building amplitude of vibration in this case. Figs. 19 and 20 reveal that the displacement patterns of the structure are nearly the same, but the structure and TMD patterns are dissimilar. The difference between Figs. 18 and 20 reveals that soil properties greatly affects the structure behavior.

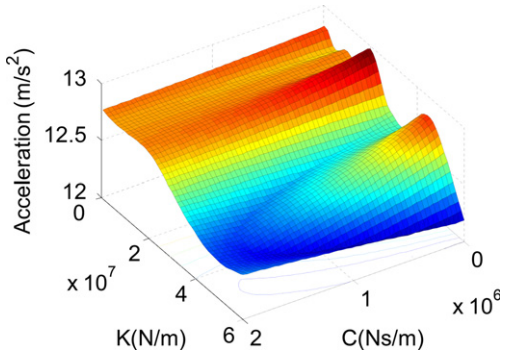

Fig. 14. The effects of TMD's C and K on $\ddot{u}_{max}$

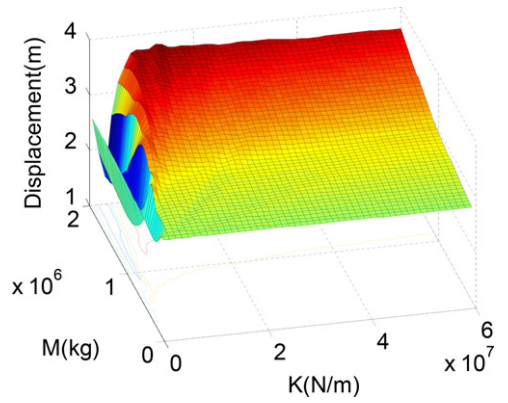

Fig. 15. The effects of TMD's M and K on u_{max}.

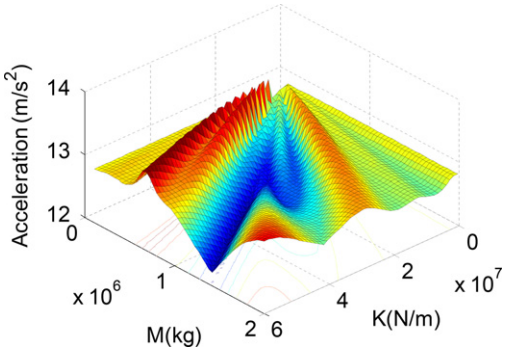

Fig. 16. The effects of TMD's M and K on $\ddot{u}_{max}$

6. Conclusions

In this paper, a mathematical model is developed to obtain the earthquake response of a high-rise building with TMD, considering SSI effects. The model is based on the time domain analysis. The ant colony optimization technique is utilized to obtain the optimum parameters for TMD. Mass, damping and spring stiffness quantities of TMD are assumed as the design variables, and the objective is to decrease the maximum displacement and acceleration of building.

The results show that the soil characteristics greatly influence on the favorite TMD parameters. It is indicated that the soil type also severely affects the time response of structures. It is also

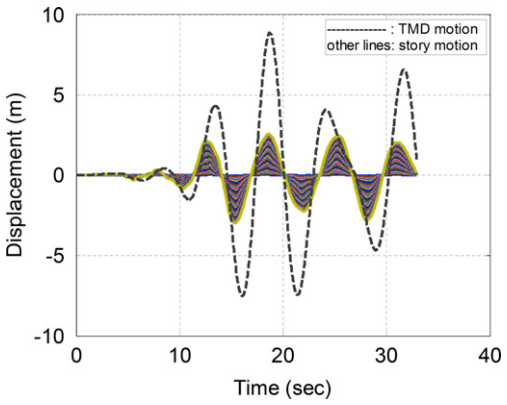

Fig. 17. Time response with TMD for soft soil.

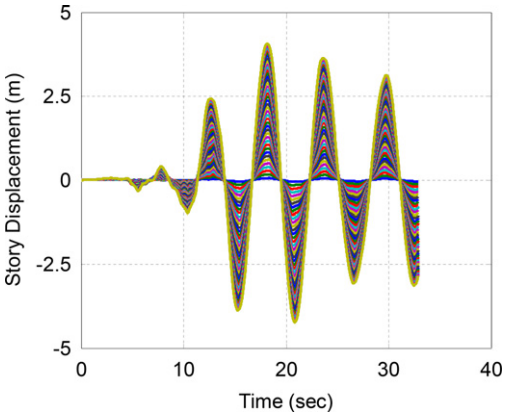

Fig. 18. Time response without TMD for soft soil.

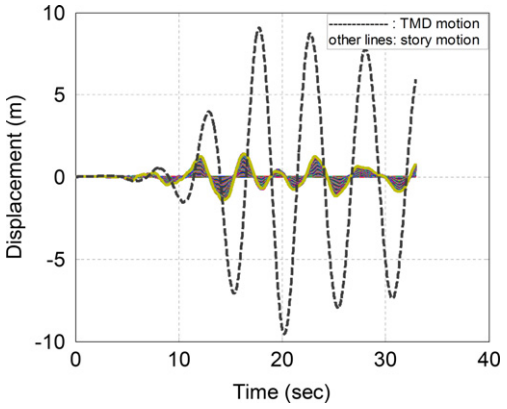

Fig. 19. Time response with TMD for dense soil.

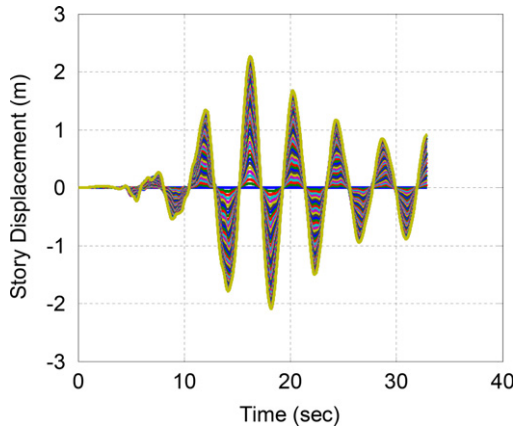

Fig. 20. Time response without TMD for dense soil.

shown that the TMDs are advantageous devices earthquake vibration mitigation of high-rise buildings. It is also implied how ACO can be employed for the design of optimum TMDs; considering soil effects. This study improves the understanding of earthquake oscillations, and helps the designers to achieve the optimized TMD for high-rise buildings.

References

[1] Villaverde R, Koyoama LA. Damped resonant appendages to increase inherent damping in buildings. Earthquake Engineering & Structural Dynamics 1993;22:491–507.
[2] Rana R, Soong TT. Parametric study and simplified design of tuned mass dampers. Journal of Engineering Structures 1998;20(3):193–204.
[3] Lin C-C, Ueng JM, Huang TC. Seismic response reduction of irregular buildings using passive tuned mass dampers. Journal of Engineering Structures 2000;22(5):513–24.
[4] Wang AP, Fung RF, Huang SC. Dynamic analysis of a tall building with a tuned-mass-damper-device subjected to earthquake excitations. Journal of Sound and Vibration 2001;244(1):123–36.
[5] Brock JE. A note on the damped vibration absorber. Journal of Applied Mechanics: ASME 1946;13:A-284.
[6] Den Hartog JP. Mechanical vibrations. fourth edition New York: McGraw-Hill; 1956.
[7] Crandall SH, Mark WD. Random vibration in mechanical systems. New York: Academic Press; 1973.
[8] Warburton GB, Ayorinde EO. Optimum absorber parameters for simple systems. Earthquake Engineering & Structural Dynamics 1980;8:197–217.
[9] Sadek F, Mohraz B, Taylor AW, Chung RM. A method of estimating the parameters of tuned mass dampers for seismic applications. Earthquake Engineering & Structural Dynamics 1997;26(6):617–35.
[10] Park J, Reed D. Analysis of uniformly and linearly distributed mass dampers under harmonic and earthquake excitation. Engineering Structures 2001;23(7):802–14.
[11] Wolf JP. Soil–structure interaction analysis in time domain. New Jersey: Prentice-Hall; 1988.
[12] Xu YL, Kwok KCS. Wind induced response of soil–structure–damper systems. Journal of Wind Engineering and Industrial Aerodynamics 1992;43(3):2057–68.
[13] Wu JN, Chen GD, Lou ML. Seismic effectiveness of tuned mass dampers considering soil–structure interaction. Earthquake Engineering & Structural Dynamics 1999;28(11):1219–33.
[14] Liu MY, Chiang WL, Hwang JH, Chu CR. Wind-induced vibration of high-rise building with tuned mass damper including soil–structure interaction. Journal of Wind Engineering and Industrial Aerodynamics 2008;96:1092–102.
[15] Wang JF, Lin CC. Seismic performance of multiple tuned mass dampers for soil–irregular building interaction systems. International Journal of Solids and Structures 2005;42(20):5536–54.
[16] Lin CC, Chang CC, Wang JF. Active control of irregular buildings considering soil–structure interaction effects. Soil Dynamics and Earthquake Engineering 2010;30(3):98–109.
[17] Lin CC, Lu LY, Lin GL, Yang TW. Vibration control of seismic structures using semi-active friction multiple tuned mass dampers. Engineering Structures 2010;32:3404–17.
[18] Li C. Effectiveness of active multiple-tuned mass dampers for asymmetric structures considering soil–structure interaction effects. Structural Design of Tall and Special Buildings 2012;21(8):543-65.
[19] Li C, Han B. Effect of dominant ground frequency and soil on multiple tuned mass dampers. Structural Design of Tall and Special Buildings 2011;20(2):151–63.
[20] Li C, Liu Y. Ground motion dominant frequency effect on the design of multiple tuned mass dampers. Journal of Earthquake Engineering 2004;8(1):89–105.
[21] Li C, Yu Z, Xiong X, Wang C. Active multiple tuned mass dampers for asymmetric structures considering soil–structure interaction. Structural Control and Health Monitoring 2010;17(4):452–72.
[22] Thomson WT, Dahleh MD. Theory of vibration with applications. 5th edition London: Prentice Hall Inc.; 1997.
[23] Newmark NM. A method of computation for structural dynamics. Journal of Engineering Mechanics (ASCE) 1959;85(EM3):67–94.
[24] Dorigo M, Gambardella LM. Ant colony system: a cooperative learning approach to the traveling salesman problem. IEEE Transactions on Evolutionary Computation 1997;1(1):53–66.
[25] Abachizadeh M, Kolahan F. Evaluating the discretization of search space in continuous problems for ant colony optimization. In: Proceedings of 37th international conference on computers and industrial engineering (CIE 37th), Alexandria, Egypt: 2007.